Direct-modulation optoelectronic oscillator for optical pulse and frequency comb generation

Brian Sinquin, Marco Romanelli, Mehdi Alouini, Marc Vallet

Direct-Modulation Optoelectronic Oscillator for Optical Pulse and Frequency Comb Generation

Brian Sinquin, Marco Romanelli, Mehdi Alouini, Marc Vallet

University of Rennes, CNRS, Institut FOTON, UMR 6082, F-35000 Rennes, France
corresponding author : marco.romanelli@univ-rennes.fr

September 3, 2024

Abstract

We report the generation of an optical pulse train with a 10 GHz repetition rate in a dual loop direct-modulation optoelectronic oscillator (OEO). Pulse generation is achieved using nonlinear compression in the OEO 5 km-long optical delay line. 3 ps pulses with a timing jitter of 13 fs are reported, while the OEO maintains a phase noise of -133 dBc/Hz at 10 kHz from the carrier. Two architectures are compared experimentally and theoretically. A frequency comb with a 1.2 THz linewidth at -30 dB is generated.

I. Introduction

Optoelectronic oscillators (OEOs) were proposed in the 90's to enhance the spectral purity of electronic microwave oscillators by utilizing optics to increase the feedback delay [1]. This delay, provided by a low loss km-long optical fiber, leads to a much higher quality factor of the oscillator, allowing for very low phase noise of the generated microwave carrier [2]. Since their invention, they have been mainly used as ultra-pure electrical frequency generators for application in telecommunication, teledetection and ranging, or sensing [3]. Alternative architectures, such as the Coupled OEO (COEO) [4] have been developed to generate short picosecond optical pulses [5, 6] allowing for a broader range of applications. Short and low jitter optical pulses at frequencies of typically 10 GHz and more have applications in optical sampling [7] or in telecommunication [8]. Pulse generation has already been demonstrated in OEOs using two different approachs : linear chirp [9] or nonlinear time-lens compression [10]. Pulses with durations ranging from a few tens of ps down to a few ps at high frequency repetition rates, are respectively achievable while showing a very low timing jitter due to the low phase noise of the OEO.

Recently, Direct-Modulation OEOs (DMOEO), i.e. OEOs based on the current modulation of the pump laser, have attracted a renewed interest [11, 12]. In particular, we recently showed that using the direct current modulation of the laser in an OEO allows for the generation of ultra-pure 10 GHz microwave signals with a very low phase noise level of -135 dBc/Hz at 10 kHz from the carrier [13] making them of interest for integration perspectives [14]. Moreover, direct current modulation of a semiconductor laser can intrinsically lead to optical pulse regimes (gain-switching [15]) at high repetition rate with durations of a few tenth of ps [16].

In this work, we implement a nonlinear compression in a DMOEO and observe the generation of picosecond pulses with low timing jitter at a 10 GHz rate. The principle relies on the interplay between the third order Kerr nonlinearity and the anomalous dispersion regime in the optical fiber delay line. The initial pulse train generated by the directly-modulated laser is amplified so that self-phase modulation [17] occurs in the optical fiber, providing a spectral broadening along with a positive chirp to the signal. The linear anomalous dispersion from the optical fiber compensates this chirp thus compressing the pulses in the temporal domain. The present article follows the plan below.

In section 2., we model and simulate both the output

signal of our DFB laser and its nonlinear compression in a 5 km-long optical fiber. Two configurations are proposed and compared. In section 3., we present two experimental implementations of the nonlinear compression in our DMOEO, which are based on the simulation results. Finally, in section 4., we extend the architecture in order to broaden the optical spectrum using a Highly NonLinear Fiber (HNLF), as an example of possible implementation.

II. Model and simulation

In order to modelize the nonlinear propagation in the OEO delay line, it is first needed to simulate the optical output signal of the directly-modulated laser. To this end, we start with the laser rate equations for the electrical field (e) and the population inversion density (n) [18]. The normalized expression of the system is given by Eq. 1 and Eq. 2 :

$$\frac{de}{dt} = \frac{1}{2}(1 - i\alpha_H)ne \tag{1}$$

$$\frac{dn}{dt} = \epsilon\left(J(t) - (1+n)(1+|e|^2)\right), \tag{2}$$

where $\epsilon = \frac{\tau_p}{\tau_c}$ is the ratio of the photon lifetime ($\tau_p = 5$ ps) and carrier lifetime ($\tau_c = 180$ ps). These equations takes into account the Linewidth Enhancement Factor (LEF) [19] ($\alpha_H = 3.8$) and the pump current $J(t) = r\,(1 + m \cdot \cos(2\pi f_0 t))$ with r being the normalized bias current, m the current modulation index, f_0 the scaled OEO oscillation frequency and t the time in units of τ_p. As the laser behaves like a PN junction, the pump current must satisfy the condition $J(t) \geq 0$. Considering the laser threshold current $i_{\text{th}} = 13$ mA, a bias current $i_0 = 60$ mA and a modulation power $P_{RF} = 20$ dBm, the laser simulation parameters reads $r = 4.6$ and $m = 1$. The intrinsic laser parameters were measured experimentally, using the well known transfer function technique for lifetimes estimation, and an original method to measure the LEF [20]. The knowledge of the former parameters allows to predict the periodic complex envelope of the optical signal produced by the laser. The optical power and instantaneous frequency of the simulated signal are shown in Fig. 1.

The gain-switching behavior due to the strong modulation causes the laser to emit a pulse train at a rate

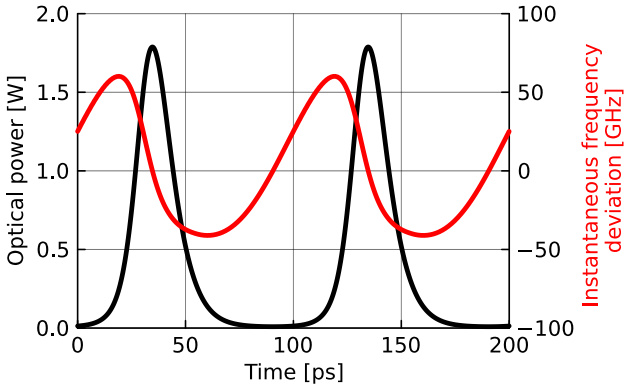

Figure 1: *Simulation of the laser output power with pump modulation. Optical power is in black, instantaneous frequency deviation in red. Pulse train period :* 100 *ps*

of 10 GHz. The generated pulses present a duration of 19 ps, an optical peak power of 1.8 W and a negative chirp caused by the LEF. The simulation of the nonlinear propagation in the delay line (SMF-28 fiber) requires to consider the optical losses ($\alpha = 0.046$ km^{-1} corresponding to 0.2 dB/km), the group velocity dispersion ($\beta_2 = -23$ ps^{2}km^{-1} corresponding to $D = 18$ ps·km^{-1}nm^{-1}) as well as the self-phase modulation ($\gamma = 1.1$ W^{-1}km^{-1}) in the optical fiber. The evolution of the optical field is governed by the NonLinear Schrödinger Equation (NLSE) whose expression is given by [17]:

$$\frac{\partial A}{\partial z} = -\frac{\alpha}{2}A - i\frac{\beta_2}{2}\frac{\partial^2 A}{\partial \tau^2} + i\gamma|A|^2 A, \tag{3}$$

where τ is the local time (the time in the frame of the pulse, moving at the group velocity in the fiber), z is the propagation distance and A is the complex envelope amplitude. Using the simulated laser output as initial condition, one can integrate the NLSE over an arbitrary length. Care has been taken to use the same phase convention (negative) in both simulations : rate equations (1-2) assume a complex field of the form $E(t) = e(t)\ e^{-i\omega_0 t}$ and the NLSE assumes a complex field of the form $E(z,t) = A(z,t)\ e^{ik_0 z}e^{-i\omega_0 t}$.

The initial chirp plays an important role in the compression mechanism. Indeed, for a positive initial chirp the fiber linear dispersion will lead to pulse compression, while for a negative initial chirp the pulse will initially spread. To control the initial chirp, in [10] a phase modulator was used to positively chirp the

laser output in order to obtain a compressed pulse at a distance of 4 km [21]. Our laser simulation shows a negatively chirped signal, which may be finely tuned in order to achieve an optimal compression at a distance of 5 km. However, the compression depends also on other parameters, i.e. the initial pulse shape and its power. Moreover, owing to the nonlinear process, changing the initial chirp may not only change the compression distance but will also change the final pulse shape, duration and peak power. For this reason, we add a tunable phase modulation to the laser output field before the nonlinear propagation in order to be able to modify its initial chirp. Fig. 2 presents a scheme of the simulated situation.

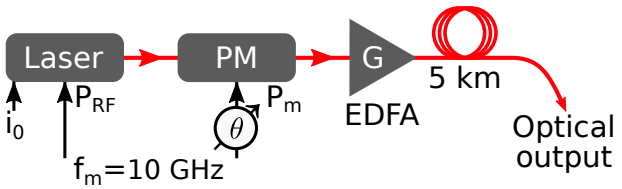

Figure 2: *Scheme of the simulated nonlinear optical transmission line.* ***PM*** *: phase modulation,* ***EDFA*** *: Erbium Doped Fiber Amplifier,* ***θ*** *: Phase-shifter. Black : electrical, Red : optical.*

The initial condition of the nonlinear propagation reads:

$$A_{in}(t) = \sqrt{\frac{P}{r-1}} \cdot e(t) \cdot e^{-i\phi_m \cos(2\pi f_m t - \theta)}, \qquad (4)$$

where $\phi_m = \pi \frac{\sqrt{2R_l P_m}}{V_\pi}$ is the phase modulation depth which depends on the half-wave voltage $V_\pi = 4.7$ V, the RF modulation power P_m at a frequency of $f_m = 10$ GHz and the load impedance $R_l = 50\ \Omega$. θ is the phase offset between the laser current modulation and the phase modulation and P is the mean optical power at the output of the fiber amplifier (see Fig. 2 EDFA).

In the following, nonlinear propagation simulations are achieved using two algorithms : symmetric Split-Step Fourier Method (SSFM) and Interaction-Picture Embedded 4th order Runge-Kutta method [22], respectively using the Julia library FiberNlse.jl [23] and a Julia implementation of the SPIP algorithm [24]. Both algorithms produced the same results on all the following simulations. For the sake of consistency with respect to the experimental parameters used later, the same laser output signal (from Fig. 1) is used in all simulations.

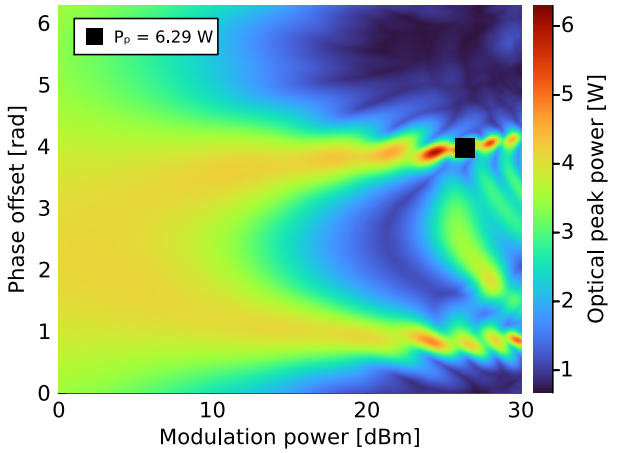

Figure 3: *Simulation : Optical peak power at the 5 km-long fiber output with respect to PM phase offset and PM power. The marker ■ represents the set of parameter for which the output optical peak power is maximized (26.4 dBm, 3.98 rad).*

In order to find the maximum pulse compression at a distance of 5 km, we simulate the system using a 2D parameter scan over the phase modulation power ($P_m \in [0, 30]$ dBm) and the phase modulation offset ($\theta \in [0, 2\pi]$ rad). The mean input optical power is set to 26 dBm as in the experiments. An ideal compression must show a reduced pulse duration and therefore an increased peak power, which we measured for each set of parameters. The optical peak power matrix is shown in Fig. 3. At the lowest phase modulation powers (0-10 dBm), the output peak power is almost constant near 4 W over a wide range of phase delays (between 1 and 4 rad) while for higher modulation powers (10-23 dBm), the optical peak power stays high only around two phase branches (1 and 4 rad), and is greatly reduced elsewhere. For powers above 23 dBm, we observe that the peak power can be increased even more locally and that moderate peak powers can be observed again between 1 and 4 rad. These results suggest that a maximum peak power compression is possible using a high phase modulation power of 26.4 dBm and that peak powers near 4 W may be obtained without using any phase modulation at all, i.e. using the native laser chirp.

In order to verify that it is possible to compress efficiently the input pulse without changing its initial chirp, we simulate the system with no phase modulation, i.e. taking $\phi_m = 0$ ($P_m = 0$ W). The propagation of the pulse along the fiber is shown on Fig. 4.

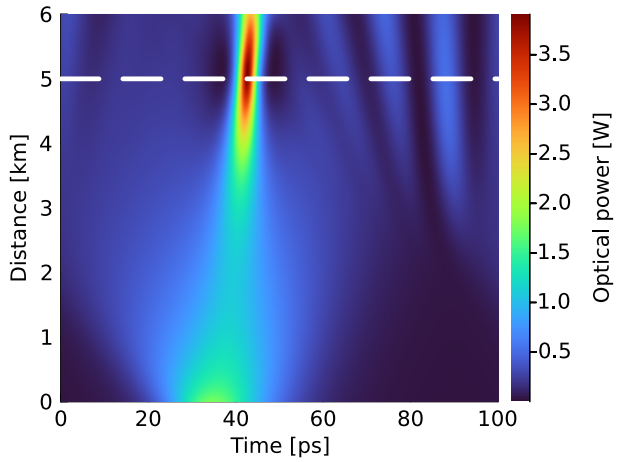

Figure 4: *Simulation of the nonlinear compression without phase modulation. Evolution of the pulse temporal profile along the fiber.*

The compression behaviour is simple in this case, the central and powerful part of the input pulse compresses, due to the interplay of GVD and SPM, towards an ideal compression point at a distance of $z = 5$ km despite the negative input chirp. The output pulse shows a 3.9 W peak power, in agreement with the low phase modulation region previously predicted in Fig. 3. Moreover, the weak power part of the input pulse spreads and interferes with the tails of adjacent pulses, resulting in parasitic oscillations around the compressed pulse, which lower the pulse quality. The output (black line) and the input (blue line) signals are compared in Fig. 5 and show an efficient compression where the output pulse duration is of 3.7 ps duration, i.e. 5 times shorter than the input duration (19 ps). This configuration is experimentally appealing as it does not require a supplementary phase modulation.

We now simulate the configuration corresponding to the maximum output peak power shown in Fig. 3, i.e by seeking $P_m = 26.4$ dBm and $\theta = 3.98$ rad in the simulation. The signal evolution is presented in Fig. 6 as a function of the propagation distance.

The simulation shows a more complex behavior,

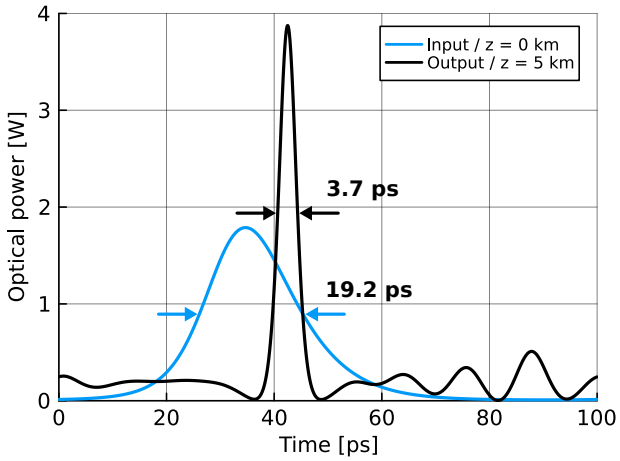

Figure 5: *Simulation of the nonlinear compression without phase modulation. Input (blue) and output at 5 km (black).*

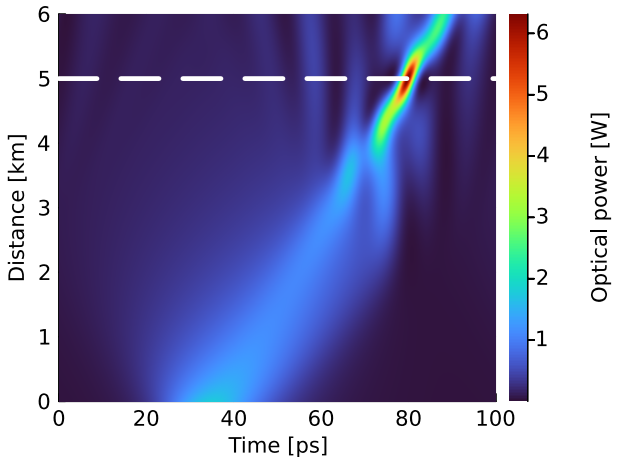

Figure 6: *Simulation of the nonlinear compression with phase modulation. Evolution of the pulse temporal profile along the fiber.*

where the initial pulse is at first spread by dispersion, then compressed at $z = 5$ km. The signal has experienced a temporal drift inside the period, due to the interplay of GVD, SPM and the initial condition (modified chirp). We also observe small residual oscillations arising from the interference of the tails of the pulse that have been spread and those of the adjacent pulses.

The input (blue line) and output (black line) signals are compared in Fig. 7 and show an efficient compression with a pulse duration of 2.7 ps and a 6.3 W peak power, corresponding to a duration division by a factor of 7 and a peak multiplication by a factor of 2.3. The pulse is surrounded by parasitic oscillations which are weaker than in the previous configuration.

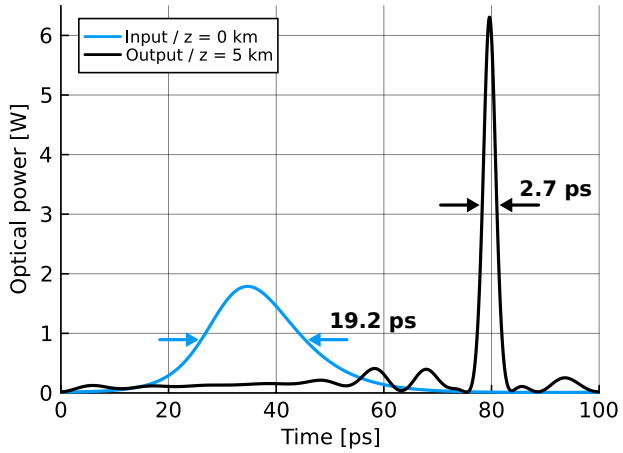

Figure 7: *Simulation of the nonlinear compression with phase modulation. Input (blue) and output at 5 km (black).*

This second configuration produces shorter and more powerful pulses, but may be more complex to realize experimentally as a supplementary phase modulation is needed. Both configurations are implemented experimentally in the next section.

It is also interesting to verify how the signal is compressed when the input chirp is perfectly compensated, i.e. when the signal is Fourier limited. It can be seen in Fig. 8 that the input signal is compressed much earlier than in previous configurations. The maximum theoretical compression for a 26 dBm mean power Fourier limited input signal is achieved at a distance of 1780 m leading to a pulse duration of 2.2 ps and a peak power of 10 W. After the pulse compresses, it decays into two sub-pulses with lower peak powers and larger durations. The quality of this pulse is higher than the previous one because of the absence of parasitic low power oscillations around it. Nevertheless, it may be difficult to perfectly compensate the initial chirp experimentally. Moreover, the durations we obtain from the other configurations (3.7 ps and 2.7 ps) are close to this one with relative differences of 68 % and 22 % respectively. Finally, a 5 km propagation distance is actually needed in order to maintain the phase noise performances of the OEO.

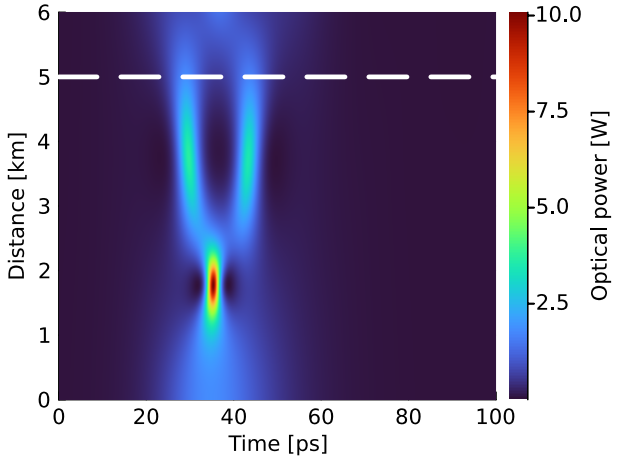

Figure 8: *Simulation: Evolution of the nonlinear compression with respect to distance, with a Fourier limited input.*

III. Experiments

The experimental architecture is sketched in Fig. 9 and is composed of the following elements. An InGaAsP/InAs DFB laser (Gooch & Housego, AA0701) emitting at 1.55 μm is directly modulated and produces optical pulses which pass through two consecutive phase modulators (iXblue Photonics, MPZ-LN-10). The first one is driven by a 100 MHz frequency synthesizer (Rohde & Schwartz, SMB 100A) and the second one by the OEO feedback signal at 10 GHz. The optical signal is amplified by an EDFA and propagates in a 5 km-long standard single-mode fiber (SMF-28). At the output of the long fiber, 90% of the signal is extracted for analysis purpose. One half of the signal is detected by a photodiode (Nortel, PP-10G) while the second part propagates 1 km further before being detected by another identical photodiode. We implement such

dual-loop architecture to further increase the spectral selectivity of the OEO due to the Vernier effect [25]. Indeed, the resonance condition must be satisfied simultaneously for the two loops, so that only the resonances which are common to both loops can oscillate. This has also a beneficial effect on the phase noise, leading to strong periodic suppression of most of the spurious tones. The two photocurrents can be delayed due to RF phase shifters before being summed, amplified and filtered around 10 GHz by a narrow-band dielectric resonator (Full Width at Half Maximum = 3.3 MHz). Part of this signal is phase shifted, amplified and fed back in the second phase modulator, while the other part is fed back to the modulation input of the laser, closing the DMOEO feedback loop. It is worth mentioning that the working point of the OEO is set by the gain nonlinearity of the last RF amplifier, whose saturation stabilizes the amplitude of the oscillation. A fraction of the feedback signal is extracted and constitutes the useful RF output.

As we use high optical powers to achieve significant SPM, Stimulated Brillouin Scattering (SBS) arises. The induced back-scattered light (depicted in Fig. 10.a) implies optical losses in the forward direction, leading to a degradation of the nonlinear compression. These transmission losses can be mitigated with an increased optical linewidth by using amplitude and/or phase modulation as sketched in Fig. 10.b. The direct modulation of the laser (orange curve) already produces amplitude and phase modulation (owing to the LEF) which leads to an increase of the SBS threshold compared to a CW signal (blue curve). We show (green curve) that an additional phase modulator (the first one in Fig. 9) driven by a 22 dBm 100 MHz signal is able to increase further the SBS threshold [26], that is enough to reduce the optical losses to the linear Rayleigh scattering limit (intrinsic losses of 0.2 dB/km).

In a first attempt to verify the simulation prediction that pulse compression is possible despite the laser chirp, we implement the system sketched in Fig. 9 without the fast phase modulation feedback loop (chirp box). We empirically searched for sets of parameters for which a pulse compression is observed at the end of the 5 km fiber. We find that for an optical power of 26 dBm, a bias current of 60 mA and a direct RF modulation power of 20 dBm, stable single-mode OEO oscillation at 10 GHz is possible along with efficient optical pulse compression.

The Auto-Correlation Function (ACF) was measured with an auto-correlator (APE, PulseCheck 150) and is presented in Fig. 11.a (blue line). The optical pulse duration is estimated to be as low as 3.3 ps when considering a sech^2 pulse profile. The ACF shows a non-zero background, with an average value of 25 %. This is compatible with a temporal signal exhibiting a low continuous background along with parasitic oscillations surrounding the pulse structure, as found in the simulations. We also compare the experimental auto-correlation functions with that calculated from the simulation result using the Wiener-Khintchine theorem (Eq. 5) :

$$I_{ACF}(\tau) = \int_{-\infty}^{+\infty} S(\nu) \cdot e^{2i\pi\nu\tau} d\nu \tag{5}$$

By adjusting the simulation parameters we are able to find good qualitative agreements with the experimental auto-correlation function in that configuration (see Fig. 11.a, dashed black line). The mean optical power was the only free parameter and was tuned to 26.4 dBm. We reproduce correctly the central part of the ACF, showing a similar pulse width, as well as the non-zero background which accounts for the presence of low intensity ripples on a whole period of the signal. The spectral domain characteristics of the optical signal is measured with a Apex Technologies AP2083A Optical Spectrum Analyzer (OSA) whose resolution bandwidth is of 400 MHz. The spectrum of the optical pulse regime (Fig. 11.b) consists in a frequency comb with a repetition frequency of 10 GHz and 310 GHz width at -30 dB, counting 31 spectral lines.

The phase noise of the detected electrical signal has been measured with a phase noise analyzer (Rohde & Schwarz, FSWP26). It is shown (red curve) in Fig. 12 and compared to the one of Ref. [13] (blue curve). The phase noise spectrum shows almost the same behavior than in [13] at high frequencies (40 kHz to 1 MHz) but an increase of about 10 dB is noticeable at lower frequencies, with a specific value of -125 dBc/Hz at 10 kHz. Phase noise spurs, which are intrinsic to OEOs, are observable at ISL frequencies of the 5 km feedback loop ($\Delta f = 40$ kHz) and periodically reduced due to the Vernier effect. The timing jitter σ_τ of this signal is computed from the phase noise as follows :

$$\sigma_\tau = \frac{1}{2\pi f_0} \sqrt{2 \int_{f_{\text{low}}}^{f_{\text{high}}} S_\phi(f)\, df}, \tag{6}$$

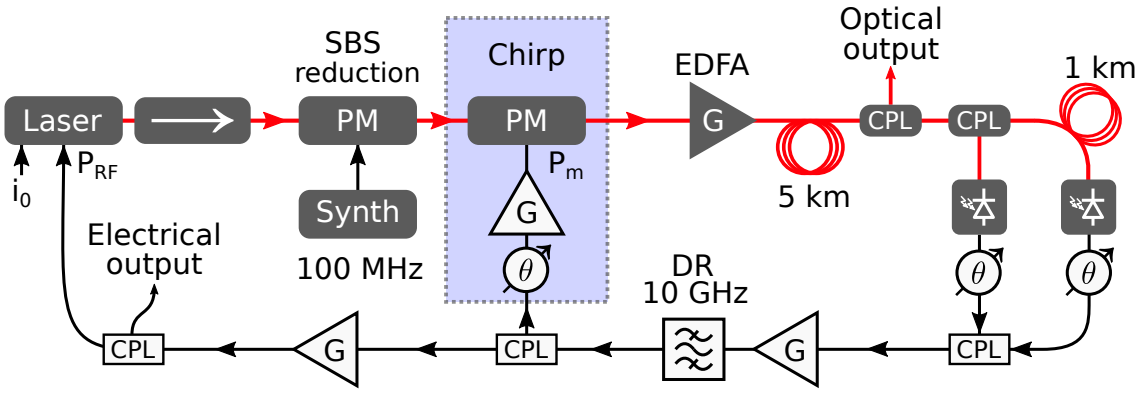

Figure 9: *Experimental setup of the pulse compression OEO with **SBS** mitigation and chirp compensation stages. **PM** : Phase modulator, **EDFA** : Erbium Doped Fiber Amplifier, **DR** : Dielectric Resonator, **θ** : Phase-shifter, **CPL** : Coupler, **Synth** : Synthesizer. Black : electrical. Red : optical.*

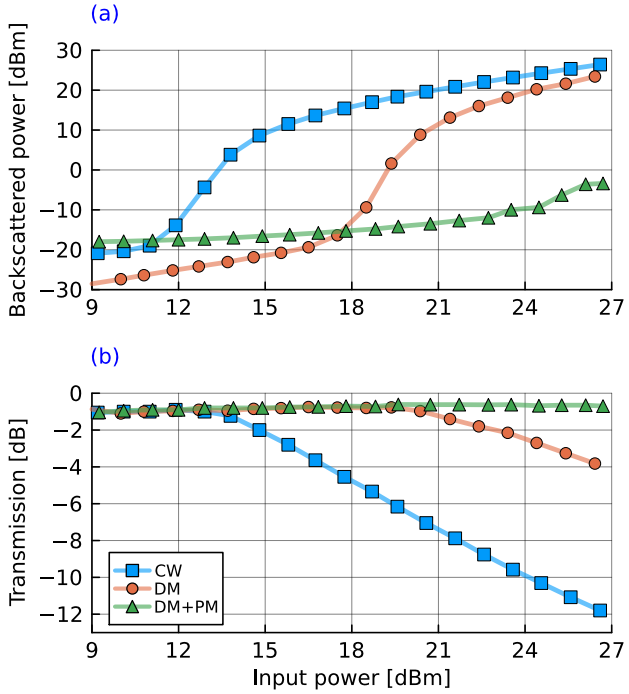

Figure 10: *Experimental characterization of the detrimental SBS effect in a 5 km SMF with respect to input power in different conditions : continuous light (squares), direct modulation (circle), direct modulation and slow phase modulation (triangle). a. Back-scattered optical power, b. Transmission. The lines are for eye guiding purpose.*

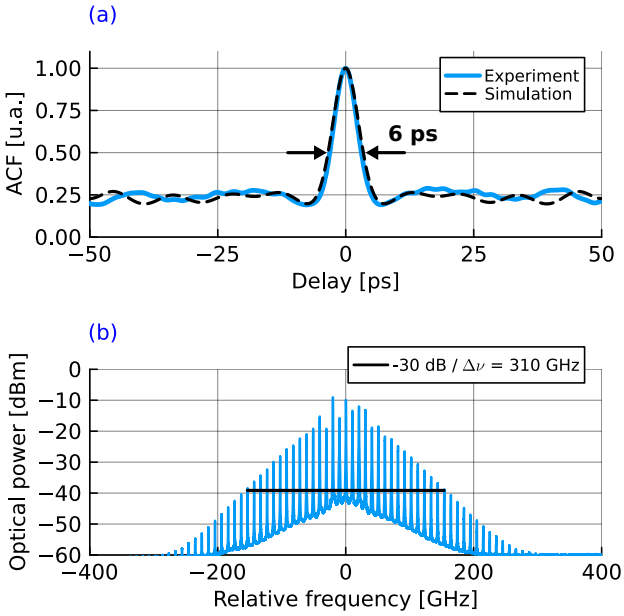

Figure 11: *Experimental characterization of the compressed optical signal at the end of the 5 km fiber. (a) Auto-correlation, (b) Optical spectrum. Blue : experimental results. Dashed black : numerical simulation. Estimated* sech^2 *pulse duration : 3.3 ps.*

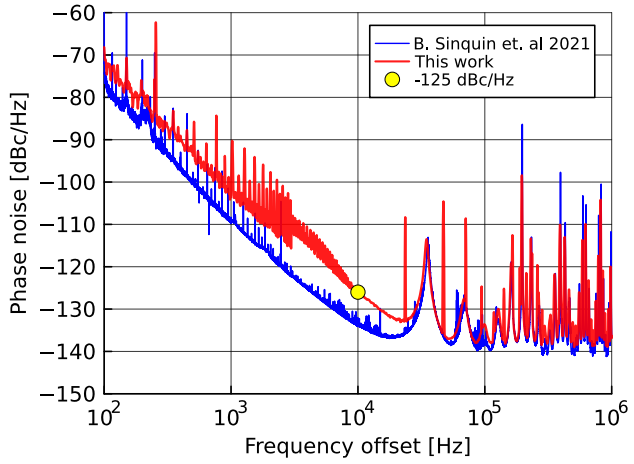

Figure 12: *Experimental phase noise measurement of the 10 GHz microwave signal (red) compared to the one measured in [13] (blue). Setup without the fast phase modulation feedback loop (chirp box).*

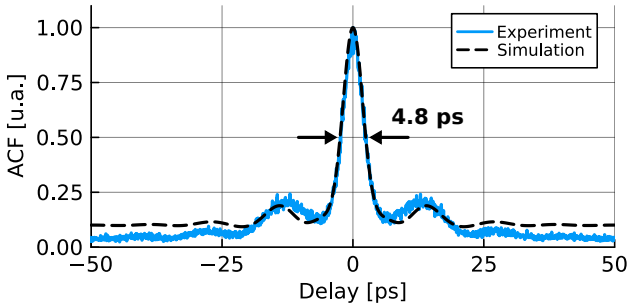

Figure 13: *Auto-correlation of the compressed optical signal at the end of the 5 km fiber. Blue : experimental, Dashed black : numerical simulation. Estimated* sech^2 *pulse duration : 3.1 ps.*

where f_0 is the oscillation frequency and $S_\phi(f)$ is the double side-band phase noise PSD [27]. The integration of the phase noise from $f_{\text{low}} = 100$ Hz to $f_{\text{high}} = 1$ MHz gives a value of 55 fs.

A second configuration is implemented where the phase modulation is used to tune the initial laser chirp. As in the previous experiment, we use an optical power of 26 dBm, a bias current of 60 mA and a direct modulation power of 20 dBm but along with a 26 dBm phase modulation power. By carefully tuning the phase shift of the phase modulation, we are able to generate stable 10 GHz OEO oscillation as well as an efficient optical pulse compression. The measured ACF (see Fig. 13, blue line) shows a pulse-like structure whose sech^2 duration is estimated to be of 3.1 ps. The ACF shows a good extinction ratio, with a reduced background compared to the previous one but with additional weak side-lobes surrounding the pulse waveform.

The numerical ACF (black dashed line) was also calculated thereby tuning the simulation parameters the mean optical power was taken to be of 26 dBm, the phase modulation power and the phase modulation phase-shift were tuned to 24.4 dBm and 3.8 rad, respectively. It shows good agreement with the measured ACF as it reproduces correctly the central part of the ACF and shows similar pulse widths. The simulated ACF also reproduces the two side lobes which account for the presence of low intensity ripples around the pulse in the time domain. Moreover, the spectrum of the optical signal is wider, i.e., 400 GHz at -30 dB, counting 40 comb lines.

Despite a higher complexity of the setup, the phase noise (see Fig. 14, red curve) shows the same levels than in [13] at high frequencies (10 kHz to 1 MHz). A level as low as -133 dBc/Hz at 10 kHz from the carrier and even lower levels at low frequencies (100 Hz) are observed, indicating a high spectral purity. These results show that the phase modulation stages and the high power nonlinear propagation are not detrimental for the spectral purity. Standard OEOs using external modulation can reach better performance with phase noise as low as -145 dBc/Hz at 10 kHz offset [28] or even -163 dBc/Hz at 6 KHz offset [2]. These performances can be reached with careful choice and optimization of all elements as well as the use of high power lasers (a DFB laser delivering a 120 mW CW signal was used in [28]) and high power photodiodes.

The integration of the phase noise from $f_{\text{low}} = 100$ Hz to $f_{\text{high}} = 1$ MHz gives a timing jitter of 13 fs. This jitter represents a period fluctuation of 130 ppm, making it compatible with optical sampling applications at 10 GHz with an Effective Number Of Bits (ENOB) of 9.96 [7].

The chirp tuning strongly depends on the variable phase-shift of the fast phase modulation, which is also affected by the two delay lines phase-shifts, so that an optimal point is somewhat tricky to find. During the empirical exploration of the parameter space, we

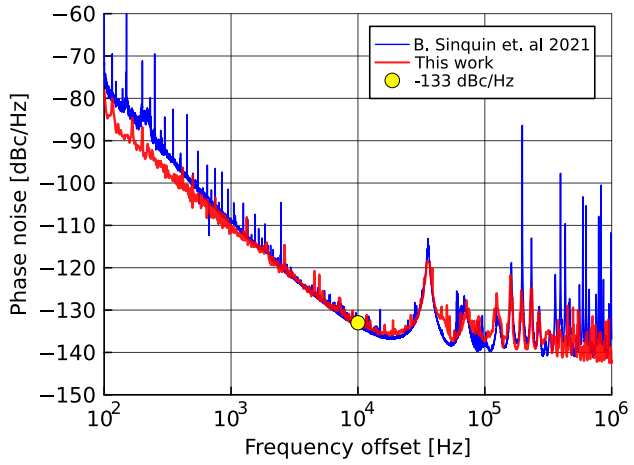

Figure 14: *Experimental phase noise measurement of the 10 GHz microwave signal (red) compared to the one measured in [13] (blue). Setup with the fast phase modulation feedback loop (chirp box).*

find that some working points exist with optimized pulse compression and degraded phase noise, meanwhile other working points exhibit optimized phase noise and degraded pulse compression. In these two experiments, the dual loop architecture is designed to enhance the spectral selectivity. However, the additional 1 km fiber introduces GVD to the compressed pulse, causing it to spread. Consequently, the two photodiodes do not detect the same optical waveform, leading to the alteration of the the interference signal. This could explain the difficulty to avoid mode hopping during tuning and to optimize both compression and phase noise at the same time. To improve the system, one should consider using a low dispersion fiber for the shorter segment, mitigating this adverse effect that could account for the observed instabilities.

IV. Application to spectral broadening

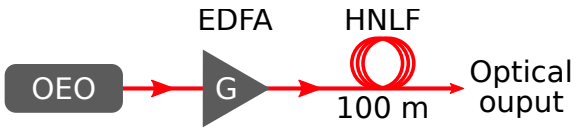

Figure 15: *Experimental setup for spectral broadening at the output of the OEO.*

We showed that nonlinear compression is possible in a DMOEO with generated pulses whose durations are as low as 3 ps. Corresponding spectra showed widths of the order of hundreds of GHz at -30 dB. For applications such as WDM telecommunication, frequency combs with a high number of spectral lines are desirable. In order to achieve a larger spectral broadening, we added a 100 m-long Highly NonLinear Fiber (HNLF) with a nonlinear factor $\gamma = 10\ \mathrm{W^{-1}km^{-1}}$ at the optical output of the OEO. With a second EDFA, we amplified the optical output pulses of the OEO as sketched in Fig. 15. We used the second experimental configuration for the OEO, and injected 26 dBm of mean optical power in the HNLF. As the specified group velocity dispersion of this fiber is very low ($|\beta_2| < 1\ \mathrm{ps^2km^{-1}}$), it is expected that only SPM affects the signal. The resulting nonlinear phase modulation broadens the optical spectrum without altering the temporal waveform, with a major dependence to optical peak power and to the pulse sharpness (duration). The auto-correlation of the 3 ps pulse at the end of the OEO is shown in Fig. 16.a.

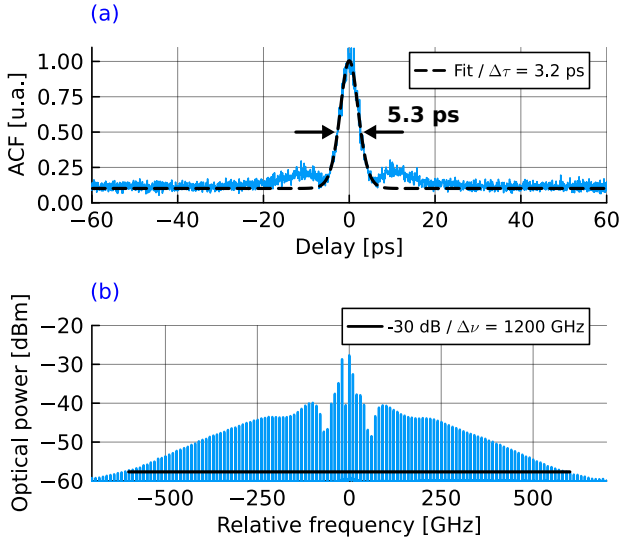

Figure 16: *Experimental characterization of the compressed optical signal at the end of the delay line. (a) Auto-correlation, (b) Optical spectrum. Estimated* sech^2 *pulse duration : 3.2 ps.*

The optical spectrum at the output of the HNLF is shown in Fig. 16.b. It has a width of 1200 GHz at -30 dB which corresponds to a frequency comb of 120 spectral lines. At -30 dB this is 3 times broader than

the output of the OEO (400 GHz).

V. Conclusions

In this paper, we have implemented nonlinear time-lens pulse compression in a direct-modulation OEO. In a first experiment, we demonstrated the generation of optical pulses as narrow as 3 ps at the end of a 5 km-long optical fiber without the need to adjust the initial chirp of the gain-switched DM laser, resulting in a simple system. In that configuration, a low timing jitter 55 fs was demonstrated, as a consequence of the good phase noise performance of the 10 GHz OEO signal (-125 dBc/Hz at 10 kHz) and despite the high power nonlinear optical propagation in the fiber. A second configuration was presented, in which the initial chirp is tuned using a phase modulator. Optical pulses of 3 ps duration were also observed, along with a greatly enhanced timing jitter of 13 fs and phase noise (-133 dBc/Hz), despite the augmented complexity of the setup. Numerical simulations were presented and supported these experimental results in both configurations, showing similar pulse ACFs and durations. To illustrate a potential application of such a device to WDM telecommunications, we injected the optical output of the pulsed DMOEO in a HNLF to broaden the spectrum, leading to a few hundreds-GHz-wide and highly coherent frequency comb. Since nonlinear compression strongly depends on medium properties and on initial conditions, the use of cleverly chosen fibers, like dispersion-compensating fibers, dispersion-shifted fibers, together with HNLF [29] or photonic crystal fibers could help to generate shorter pulses, wider spectra and potentially octave-spanning supercontinuums [30]. Moreover, a specific design of the compression could allow for a precise control of the pulse shape or for flat frequency comb generation.

Acknowledgments

We thank Arnaud Fernandez and Goulc'hen Loas for fruitful discussions.

Funding

This research was funded by Agence Nationale de la Recherche (ANR), grant number 22-PEEL-0008 (PEPR Électronique - ORORE) and Région Bretagne, FEDER, Rennes Métropole (CPER PhotBreizh).

Disclosure

The authors declare no conflicts of interest.

Data availability

Data underlying the results presented in this paper are not publicly available at this time but may be obtained from the authors upon reasonable request.

References

[1] X. S. Yao and L. Maleki, "Optoelectronic microwave oscillator," *Journal of the Optical Society of America B*, vol. 13, no. 8, p. 1725, aug 1996.

[2] D. Eliyahu, D. Seidel, and L. Maleki, "RF Amplitude and Phase-Noise Reduction of an Optical Link and an Opto-Electronic Oscillator," *IEEE Trans. Microw. Theory Tech.*, vol. 56, no. 2, pp. 449–456, 2008.

[3] T. Hao, Y. Liu, J. Tang, Q. Cen, W. Li, N. Zhu, Y. Dai, J. Capmany, J. Yao, and M. Li, "Recent advances in optoelectronic oscillators," *Advanced Photonics*, vol. 2, no. 04, p. 1, jul 2020.

[4] X. Yao, L. Davis, and L. Maleki, "Coupled optoelectronic oscillators for generating both RF signal and optical pulses," *Journal of Lightwave Technology*, vol. 18, no. 1, pp. 73–78, jan 2000.

[5] E. Salik, N. Yu, and L. Maleki, "An Ultralow Phase Noise Coupled Optoelectronic Oscillator," *IEEE Photonics Technology Letters*, vol. 19, no. 6, pp. 444–446, mar 2007.

[6] Y. K. Chembo, D. Brunner, M. Jacquot, and L. Larger, "Optoelectronic oscillators with time-delayed feedback," *Reviews of Modern Physics*, vol. 91, no. 3, p. 035006, sep 2019.

[7] G. C. Valley, "Photonic analog-to-digital converters," *Optics Express*, vol. 15, no. 5, p. 1955, mar 2007.

[8] G. P. Agrawal, *Fiber-Optic Communication Systems*. Wiley, oct 2010.

[9] Z. He, L. Li, J. Zhang, and J. Yao, "Low jitter microwave pulse train generation based on an optoelectronic oscillator," *Optics Express*, vol. 29, no. 21, p. 33491, oct 2021.

[10] Y. K. Chembo, A. Hmima, P. A. Lacourt, L. Larger, and J. M. Dudley, "Generation of Ultralow Jitter Optical Pulses Using Optoelectronic Oscillators With Time-Lens Soliton-Assisted Compression," *Journal of Lightwave Technology*, vol. 27, no. 22, pp. 5160–5167, 2009.

[11] C. D. Muñoz, M. Varón, F. Destic, and A. Rissons, "Self-starting vcsel-based optical frequency comb generator," *Optics Express*, vol. 28, no. 23, pp. 34 860–34 874, 2020.

[12] J. H. T. Mbé, M. C. Njidjou, A. F. Talla, P. Woafo, and Y. K. Chembo, "Multistability, relaxation oscillations, and chaos in time-delayed optoelectronic oscillators with direct laser modulation," *Optics Letters*, vol. 49, no. 5, pp. 1277–1280, 2024.

[13] B. Sinquin, M. Romanelli, S. Bouhier, L. Frein, M. Alouini, and M. Vallet, "Low Phase Noise Direct-Modulation Optoelectronic Oscillator," *Journal of Lightwave Technology*, vol. 39, no. 24, pp. 7788–7793, dec 2021.

[14] J. Tang, T. Hao, W. Li, D. Domenech, R. Baños, P. Muñoz, N. Zhu, J. Capmany, and M. Li, "Integrated optoelectronic oscillator," *Optics Express*, vol. 26, no. 9, p. 12257, apr 2018.

[15] D. M. Pataca, P. Gunning, M. L. Rocha, J. K. Lucek, R. Kashyap, K. Smith, D. G. Moodie, R. P. Davey, R. F. Souza, and A. S. Siddiqui, "Gain-Switched DFB Lasers," *Journal of Microwaves and Optoelectronics*, vol. 1, no. 1, 1997.

[16] C. D. Muñoz, A. Rissons, F. Destic, J. C. Rico, and M. Varón, "VCSEL Based Optoelectronic Oscillator (VBO) for 1.25 Gbit/s RZ Pulse Optical Data Generation," in *MWP 2018 - 2018 International Topical Meeting on Microwave Photonics*. Institute of Electrical and Electronics Engineers Inc., nov 2018.

[17] G. Agrawal, *Nonlinear Fiber Optics*. Elsevier, 2013.

[18] T. Erneux and P. Glorieux, *Laser Dynamics*. Cambridge University Press, apr 2010, vol. 148.

[19] C. Henry, "Theory of the linewidth of semiconductor lasers," *IEEE Journal of Quantum Electronics*, vol. 18, no. 2, pp. 259–264, feb 1982.

[20] B. Sinquin and M. Romanelli, "Determination of the linewidth enhancement factor of semiconductor lasers by complete optical field reconstruction," *Optics Letters*, vol. 48, no. 4, p. 863, feb 2023.

[21] M. Hanna, P.-A. Lacourt, S. Poinsot, and J. M. Dudley, "Optical pulse generation using soliton-assisted time-lens compression," *Optics Express*, vol. 13, no. 5, p. 1743, mar 2005.

[22] S. Balac and F. Mahé, "Embedded runge–kutta scheme for step-size control in the interaction picture method," *Computer Physics Communications*, vol. 184, no. 4, pp. 1211–1219, 2013.

[23] B. Sinquin, "Fibernlse.jl," Aug. 2023.

[24] S. Balac and A. Fernandez, "Spip: A computer program implementing the interaction picture method for simulation of light-wave propagation in optical fibre," *Computer Physics Communications*, vol. 199, pp. 139–152, 2016.

[25] X. Yao, L. Maleki, Yu Ji, G. Lutes, and Meirong Tu, "Dual-loop opto-electronic oscillator," in *Proceedings of the 1998 IEEE International Frequency Control Symposium (Cat. No.98CH36165)*. IEEE, 1998, pp. 545–549.

[26] A. Kobyakov, M. Sauer, and D. Chowdhury, "Stimulated Brillouin scattering in optical fibers," *Advances in Optics and Photonics*, vol. 2, no. 1, p. 1, mar 2010.

[27] E. Rubiola, *Phase Noise and Frequency Stability in Oscillators*, 1st ed., ser. RF and microwave engineering. The Edinburgh Building, Cambridge CB2 8RU, UK: Cambridge University Press, nov 2008.

[28] O. Lelievre, V. Crozatier, P. Berger, G. Baili, O. Llopis, D. Dolfi, P. Nouchi, F. Goldfarb, F. Bretenaker, L. Morvan, and G. Pillet, "A model for designing ultralow noise single- and dual-loop 10-GHz optoelectronic oscillators," *J. Light. Technol.*, vol. 35, no. 20, pp. 4366–4374, 2017.

[29] P. M. Anandarajah, R. Maher, Y. Q. Xu, S. Latkowski, J. O'Carroll, S. G. Murdoch, R. Phelan, J. O'Gorman, and L. P. Barry, "Generation of Coherent Multicarrier Signals by Gain Switching of Discrete Mode Lasers," *IEEE Photonics Journal*, vol. 3, no. 1, pp. 112–122, feb 2011.

[30] J. M. Dudley, G. Genty, and S. Coen, "Supercontinuum generation in photonic crystal fiber," *Reviews of Modern Physics*, vol. 78, no. 4, pp. 1135–1184, oct 2006.